nature materials

LETTERS

PUBLISHED ONLINE: 11 JULY 2010 | DOI: 10.1038/NMAT2792

Multimaterial piezoelectric fibres

S. Egusa[1], Z. Wang[1,2], N. Chocat[3], Z. M. Ruff[3], A. M. Stolyarov[1,4], D. Shemuly[3], F. Sorin[1,3], P. T. Rakich[1†], J. D. Joannopoulos[1,2] and Y. Fink[1,3]*

Fibre materials span a broad range of applications ranging from simple textile yarns to complex modern fibre-optic communication systems. Throughout their history, a key premise has remained essentially unchanged: fibres are static devices, incapable of controllably changing their properties over a wide range of frequencies. A number of approaches to realizing time-dependent variations in fibres have emerged, including refractive index modulation[1–4], nonlinear optical mechanisms in silica glass fibres[5–8] and electroactively modulated polymer fibres[9]. These approaches have been limited primarily because of the inert nature of traditional glassy fibre materials. Here we report the composition of a phase internal to a composite fibre structure that is simultaneously crystalline and non-centrosymmetric. A ferroelectric polymer layer of 30 μm thickness is spatially confined and electrically contacted by internal viscous electrodes and encapsulated in an insulating polymer cladding hundreds of micrometres in diameter. The structure is thermally drawn in its entirety from a macroscopic preform, yielding tens of metres of piezoelectric fibre. The fibres show a piezoelectric response and acoustic transduction from kilohertz to megahertz frequencies. A single-fibre electrically driven device containing a high-quality-factor Fabry–Perot optical resonator and a piezoelectric transducer is fabricated and measured.

A promising path for introducing rapid modulation into fibres would be through the piezoelectric effect[10,11]. Embedding piezoelectric domains that would be poled in the fibre's cross-section would allow fibres to be electrically actuated over broad frequencies on the one hand, and to function as sensitive broadband microphones on the other. However, fibres for the most part have been made of materials in the disordered glassy state precluding the symmetry requirements for piezoelectricity. Moreover, the need to apply electric fields to the piezoelectric material necessitates the formation of conducting electrodes, and doing so in the fibre cross-section direction presents significant processing challenges.

Recent progress in drawing of fibres made of a multiplicity of materials[12] presents new opportunities for addressing precisely such a challenge involving a wide disparity of length scales. With this approach, fibre materials are drawn from preforms in a regime dominated by viscous forces allowing for internal low-viscosity domains to be arranged in non-equilibrium cross-sections confined by viscous glassy boundary layers. At first it may seem that a simple solution exists to this problem: constructing a piezoelectric fibre could be accomplished in a straightforward manner by assembling a preform made of poly(vinylidene fluoride) (PVDF; refs 13,14), with metal electrodes and an insulating polymer, which would be followed by a thermal draw. The stress present during the fibre draw should in principle induce the nonpolar α to the ferroelectric β phase transition in the PVDF layer[13,15,16]; moreover, one can then use the internal metal wires to pole the PVDF layer. However, on detailed examination, a number of challenges and seemingly conflicting requirements emerge, which span a wide range of length scales. On the hundreds of micrometres level, the necessity to use crystalline materials both for the piezoelectric layer and the electrical conductors leads to the formation of multiple adjacent low-viscosity domains of high aspect ratio. These domains undergoing a significant reduction in cross-sectional dimensions (during the fibre draw) are susceptible to capillary break-up and mixing resulting from flow instabilities[17]. At the tens of micrometres level, layer thickness variations either in the lateral or in the longitudinal directions[17,18] preclude the formation of the coercive field needed for poling. Finally, on the length scale of the molecular spacing, even if capillary break-up were kinetically averted and uniform sections of fibres at metre lengths were to emerge they would not exhibit piezoelectricity because the stress and strain conditions necessary to induce the thermodynamic phase transition in PVDF cannot be sustained in the fibre draw process leading to a nonpolar phase.

To address these challenges, two materials with unusual properties are necessary. The first is a material that is simultaneously viscous and conductive. Carbon-loaded poly(carbonate) (CPC) is a good candidate, exhibiting both high viscosity (10^5–10^6 Pa s) at the draw temperature and adequate conductivity (1–10^4 Ω m) over the frequency range from d.c. to tens of megahertz. Incorporating CPC into the fibre structure serves to facilitate short-range (hundreds of micrometres) charge transport on length scales associated with the fibre cross-section and confine the low-viscosity crystalline piezoelectric layer during the draw process. The second is a material that crystallizes directly into the piezoelectric phase. Poly(vinylidene-fluoride-trifluoroethylene) copolymer (P(VDF-TrFE); ref. 19) assumes the ferroelectric β phase spontaneously on solidification from the melt[20,21] without necessitating any mechanical stress, making it particularly suitable for the thermal fibre drawing process.

The constituent fibre materials are then assembled as illustrated in Fig. 1a. A series of shells comprising a 700-μm-thick layer of P(VDF-TrFE) (70:30 molar ratio, Solvey; melt-pressed from pellets) and 250-μm-thick layers of CPC are assembled with indium filaments and a poly(carbonate) cladding. The entire structure is consolidated at 210 °C to remove trapped gas and form high-quality interfaces. The preform is then thermally drawn in a furnace at 230 °C into fibres more than 100 m long. Scanning

[1]Research Laboratory of Electronics, Massachusetts Institute of Technology, 77 Massachusetts Avenue, Cambridge, Massachusetts 02139, USA, [2]Department of Physics, Massachusetts Institute of Technology, 77 Massachusetts Avenue, Cambridge, Massachusetts 02139, USA, [3]Department of Materials Science and Engineering, Massachusetts Institute of Technology, 77 Massachusetts Avenue, Cambridge, Massachusetts 02139, USA, [4]School of Engineering and Applied Sciences, Harvard University, 29 Oxford Street, Cambridge, Massachusetts 02138, USA. †Present address: Sandia National Laboratories, PO Box 5800, Albuquerque, New Mexico 87185, USA. *e-mail: yoel@mit.edu.

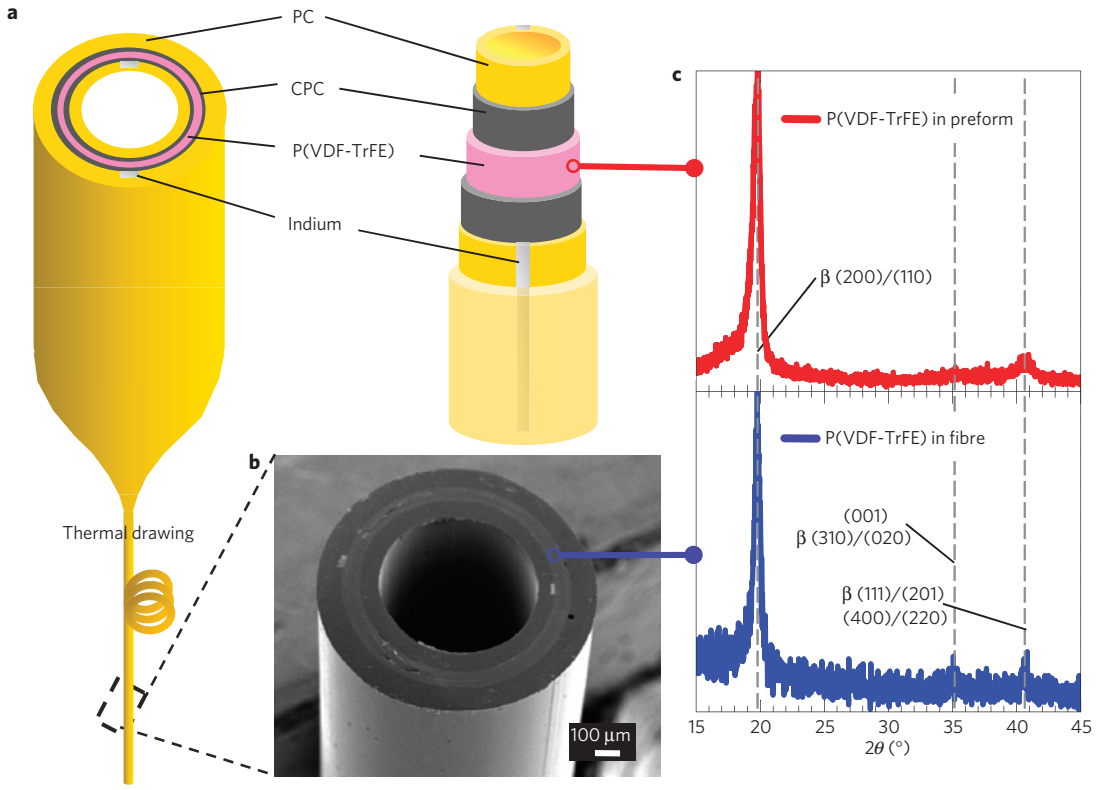

Figure 1 | Structure of piezoelectric fibres. a, Schematic of the fabrication process of a cylindrical piezoelectric fibre. A preform is constructed by consolidating a shell of P(VDF-TrFE), shells containing CPC/indium electrodes and poly(carbonate) (PC) cladding. **b**, SEM micrograph of the cross-section of a cylindrical piezoelectric fibre. **c**, XRD patterns of P(VDF-TrFE) samples extracted from drawn fibres and taken from melt-pressed films used in the preforms. The diffraction peaks indicate β-phase P(VDF-TrFE).

electron microscopy (SEM) images of the fibre cross-section show the P(VDF-TrFE) layer (40 µm thick) sandwiched between CPC layers, with the shape and the aspect ratio unchanged from those of the preform (Fig. 1b). Wide-angle X-ray diffraction (XRD) measurements of P(VDF-TrFE) copolymer domains harvested from the drawn fibres are compared to the neat material used for the preforms. Both specimens exhibit identical peaks at $2\theta = 19.9°$, 35.2° and 40.7°, which correspond to (200)/(110), (001) and (310)/(020), (111)/(201) and (400)/(220) peaks of the β phase[22], respectively (Fig. 1c), thus establishing that the drawn copolymer solidifies in its β phase. The crystallinity fraction as calculated from XRD patterns is over 90%. The obtained fibre is then poled by applying through the internal fibre electrodes an electric field in excess of 60 MV m^{-1}, which is above the literature value[23] of coercive fields. Long lengths of fibres are readily poled in this way.

To unequivocally establish that the internal copolymer layer was macroscopically poled we adopt a two-step approach. First, we show that the internal piezoelectric modulation indeed translates to a motion of the fibre's surface using a heterodyne optical vibrometer[24,25] at kilohertz frequencies where the fibre dimension is much smaller than the acoustic wavelength. Second, we proceed to an acoustic wave measurement at megahertz frequencies where the fibre dimension exceeds the wavelength and the fibre geometry alters the acoustic wavefront. In the first step, the fibre sample is electrically driven by a sine wave with the amplitude of 10 V. The vibrating fibre surface serves as an oscillating reflector and Doppler-shifts the frequency of the reflected light (Fig. 2a), yielding frequency-modulation side bands spaced at the modulation frequency ω_D. The amplitudes of the side bands are proportional to the velocity amplitude of the vibration. Figure 2b shows the observed side bands from the cylindrical fibre of Fig. 1, driven at frequencies from 1.3 to 1.9 kHz, thereby establishing a macroscopic piezoelectric response from the embedded ferroelectric layers. The side-band amplitude modulation response is found at ∼−60 dB below the main beat tone around these frequencies. Figure 2c shows the same frequency-modulation side bands for a rectangular fibre with an embedded planar piezoelectric layer, fabricated using a technique similar to the one described above (see Supplementary Information). The rectangular geometry couples more efficiently to the optical beam, leading to a marked improvement in the signal measured in the side bands compared with the immediate background. It also leads to a 20 dB increase in the side-band amplitude with respect to the heterodyne subcarrier. The ability to optimize the external fibre geometry with respect to the measurement system and application is another compelling property of this approach.

The fibre draw is realized in a stress and temperature regime dominated by viscous forces (as opposed to surface tension) allowing for non-circular geometries to be realized. Controlling the precise shape of the fibre allows one in principle to tailor the acoustic wavefront and its associated radiation pattern in the high-frequency limit where the acoustic wavelength is smaller than the lateral dimension of the fibre. Figure 2d illustrates the result of finite-element calculation of the acoustic wavefront emanating from three distinct fibre geometries. As shown, the fibre structure and its associated acoustic wavefront share the same symmetry elements.

We follow with direct acoustic measurements, using the fibres both as an acoustic sensor and as an acoustic actuator centred at 1 MHz. Such a frequency range is typical in ultrasound imaging applications. A schematic of the set-up is shown in Fig. 3a. A water-immersion ultrasonic transducer (Olympus Panametrics-NDT, 1.0 MHz-centred) is coupled to a fibre sample across a water tank to match the acoustic impedance. The fibre sample is

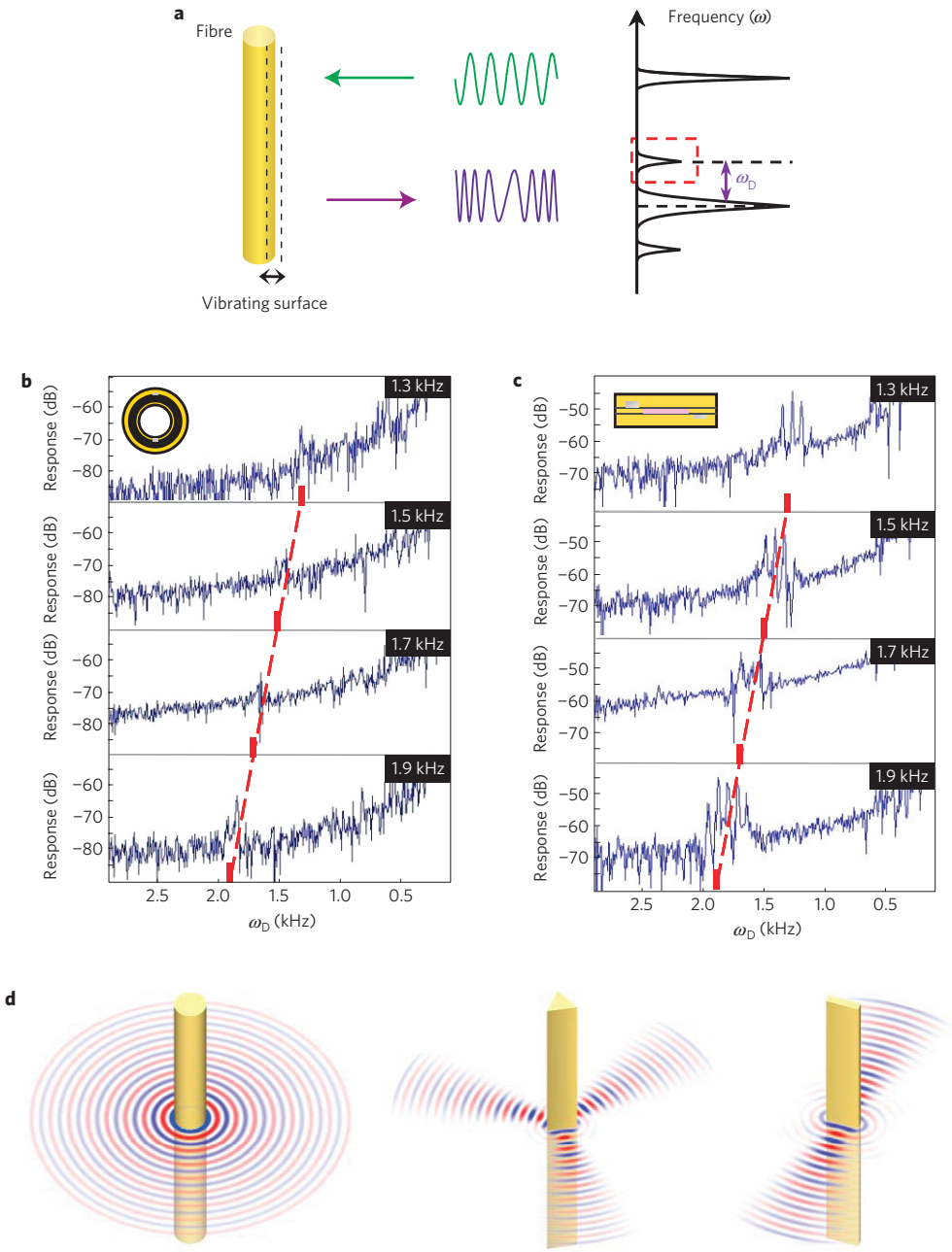

Figure 2 | Acoustic emission from piezoelectric fibres. a, Schematics of the laser Doppler vibrometer used to characterize the speed and frequency of the surface vibration of a fibre modulated at frequency ω_D. **b**,**c**, Measured frequency-modulation side bands as a function of ω_D for piezoelectric fibres with cylindrical and rectangular cross-sections, respectively. The frequency range is illustrated in **a** as a red rectangle. **d**, Near-field pressure patterns of the acoustic emission at 1.3 MHz from a circular fibre, a triangular fibre and a rectangular fibre with cross-sectional dimensions about 2 mm.

attached to the water tank surface through immersion gel, with the piezoelectric layer facing towards the transducer. The rectangular geometry further improves the acoustic directionality. At megahertz frequencies, capacitive electromagnetic coupling between the transducer circuit and the receiver charge amplifier can be significant even with careful shielding and grounding[26]. To separate the acoustic signals from the electromagnetic interference, we use a pulsed excitation and time-gate the received signals, exploiting the five orders of magnitude difference in the propagation speed between acoustic and electromagnetic pulses. The temporal traces of the amplified voltages under a pulsed excitation are measured with a carrier frequency at 600 kHz and a 52 μs temporal envelope at a 6.5 kHz repetition rate. The time delay of the received pulses is consistent with acoustic propagation in water at $1{,}470 \pm 30\ \mathrm{m\,s^{-1}}$ (Fig. 3b). Frequency-domain characterizations of the flat rectangular piezoelectric fibres are carried out with a fixed transducer-to-fibre distance, with the pulsed excitation and the time-gated signal processing (Fig. 3c). The measured piezoelectric response of the fibre, both as a sensor and an actuator, essentially follows the intrinsic frequency profile of the transducer. Although the frequency range is limited here by the bandwidth of the transducer, polymeric piezoelectric elements are in principle broadband and the piezoelectric fibres could operate at a far broader range of frequencies. For example, similar fibres were used to generate audible sound between 7 kHz and 15 kHz with a driving voltage of 5 V.

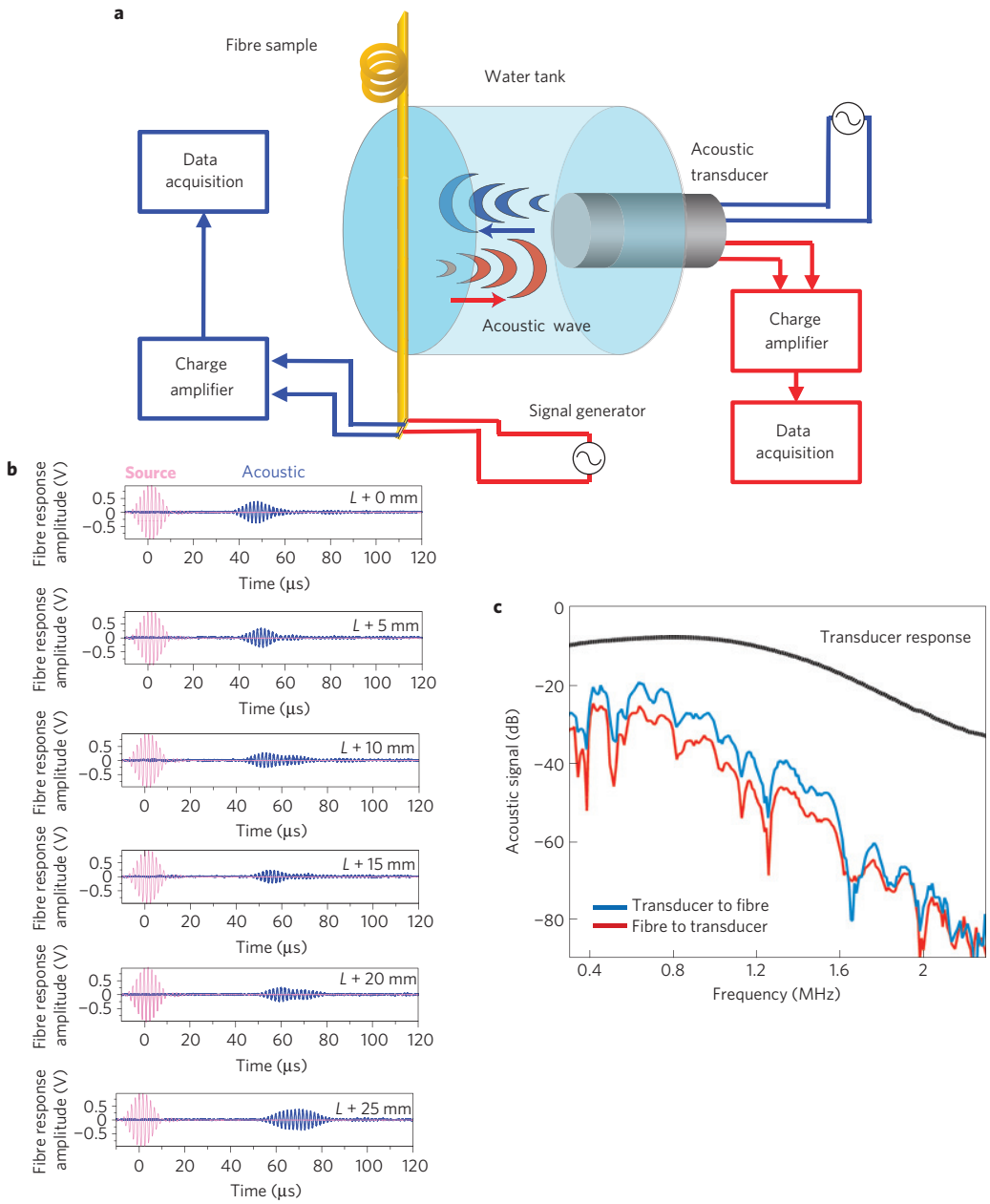

Figure 3 | Acoustic transmission characterization. a, Experimental set-up for acoustic characterization of piezoelectric fibres. An acoustic wave travels across a water tank from a water-immersion acoustic transducer to a fibre sample, and vice versa. **b**, Temporal traces of electrically amplified acoustic signals detected by a piezoelectric fibre, shown together with the excitation signals, where *L* is the starting distance between the transmitter and the receiver. **c**, Acoustic signal detected (blue curve) and emitted (red curve) by a piezoelectric rectangular fibre around 1 MHz. The dotted line is the power spectrum of the (1 MHz-centred) transducer used.

The potential to modulate sophisticated optical devices is illustrated by constructing a fibre with a Fabry–Perot optical cavity structure[1,3] layered on an embedded piezoelectric element. The fabrication process is shown in Fig. 4a. SEM images show that the piezoelectric Fabry–Perot rectangular fibre (Fig. 4b) is 800 μm wide and exhibits a well-maintained preform-to-fibre dimensional ratio and adhesion of the structures. Reflectivity of the piezoelectric Fabry–Perot fibre is characterized with a Fourier transform infrared microscope (Bruker Optics, Tensor/Hyperion 1,000), revealing the reflectivity reaching 90% around 1,500 nm (Fig. 4c, inset). The spectral dip associated with the Fabry–Perot resonant mode is identified at 1,550 nm. We again use heterodyne interferometry to characterize the fibre vibration produced by the embedded piezoelectric element. In Fig. 4c, the piezoelectric Fabry–Perot fibre is electrically driven by a sine wave at frequencies stepped from 1.5 to 8.5 kHz with the amplitude of 10 V, and the probe beam is focused on the Fabry–Perot structure to take advantage of the enhanced reflection from the bulk structure (see Supplementary Information). The variation of the side-band amplitude in Fig. 4c suggests signals enhanced or dampened by underlying acoustic resonances of the fibre sample. These piezoelectric Fabry–Perot fibres are mechanically robust and yet flexible, and can be assembled into a fabric for large area coverage as shown in Fig. 4d. The manifested colour of the fabric is the reflection from the third-order band of the Fabry–Perot optical structure embedded in the fibres.

Monolithic processing of piezoelectric transducers in fibre form presents opportunities in a variety of applications that take advantage of the fibre's elongated geometry. The large aspect ratio

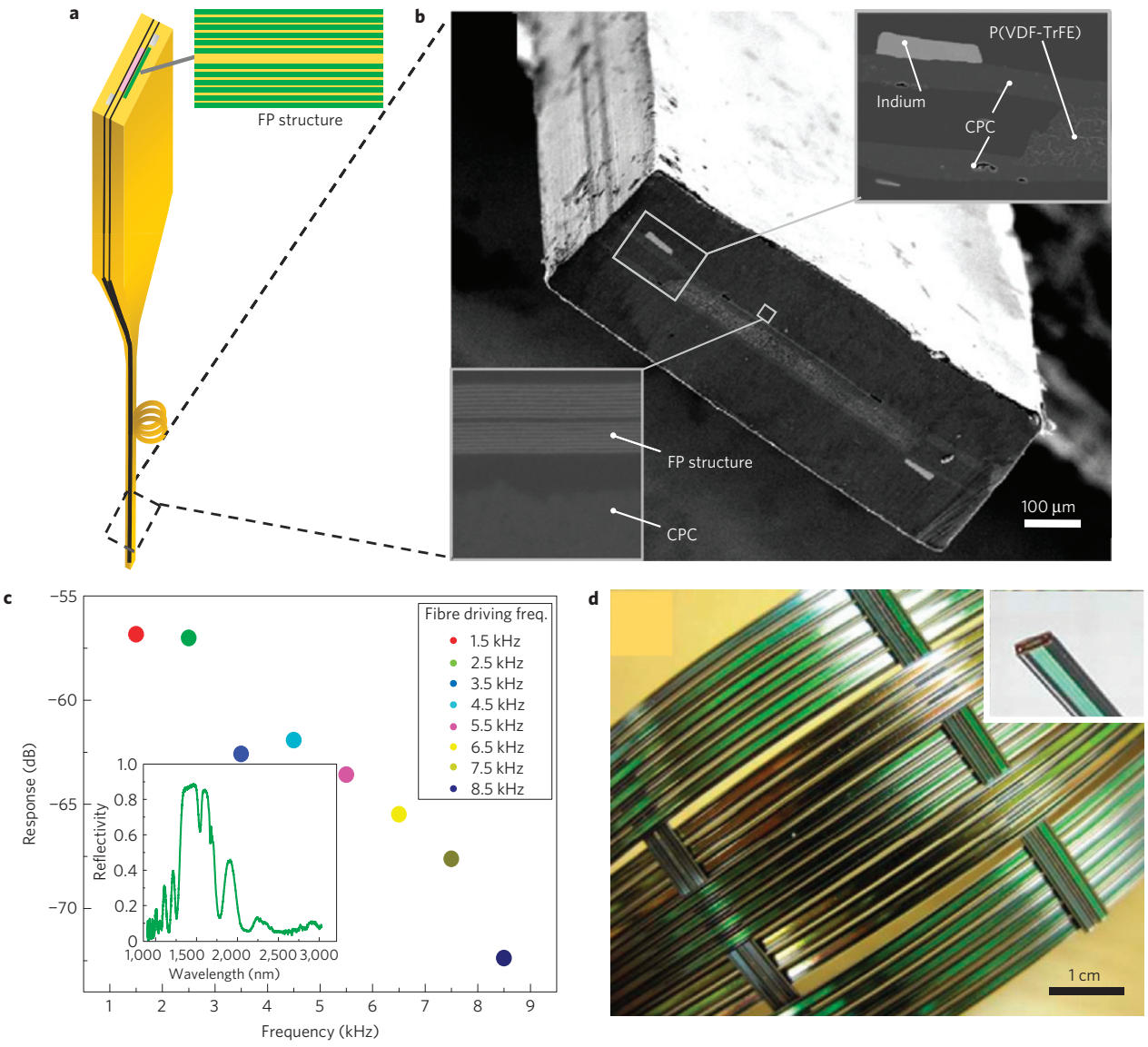

Figure 4 | Integrated piezoelectric-modulated optical fibre. a, Schematic of the fabrication process of an integrated piezoelectric Fabry–Perot (FP) rectangular fibre. A Fabry–Perot optical cavity is embedded with the piezoelectric structure in a preform. The preform is thermally drawn into a microstructured fibre. **b**, SEM micrograph of the cross-section of an integrated piezoelectric Fabry–Perot fibre. **c**, Side-band amplitude of the frequency-modulated optical reflection from a FP fibre, substantiating the prospect of optical modulation in piezoelectric fibres. The fibre is characterized with the fibre-optic heterodyne interferometer. Inset: Reflection spectrum of the piezoelectric Fabry–Perot fibre measured with Fourier transform infrared spectroscopy. **d**, Two-dimensional device fabric constructed by knitting the piezoelectric/Fabry–Perot fibres as threads. Inset: Photograph of an individual fibre.

of the piezoelectric fibre devices could form the basis for an active catheter capable of accurate pressure and flow measurements in very small blood vessels (inter-cranial), *in vivo* endovascular imaging and acoustic microscopy inside acoustically opaque organs[27]. Uniform piezoelectric fibres of tens of metres have been prepared, with potential for distributed sensing[12]: their sensitivity to stress and strain combined with their low profile makes them ideal for constructing minimally perturbative (sparse) sensor meshes for studying large-area distributions of the pressure and velocity fields in myriads of fluid flow applications including oceanic current monitoring[11]. Finally, fabrics woven from piezoelectric fibres could be used as a communication transceiver[28]. In addition, the capability of fabricating acoustic fibres with arbitrary cross-sections allows for integrating additional ferroelectric functionalities in a single-fibre device, such as energy conversion[29,30] and other actively modulated devices[29].

Methods

Acoustic transmission measurement. The rectangular fibre sample used in the measurement for Fig. 3 has a lateral dimension of 3 mm, approximately twice that of the acoustic wavelength at 1 MHz. In this context, a rectangular fibre would show stronger directionality than that of a circular fibre. A 30-mm-long section of the fibre under test is coupled to the water tank through ultrasound gel. The transducer-to-fibre distance is roughly 97 mm, approximately 70 acoustic wavelengths at 1 MHz.

Received 18 January 2010; accepted 27 May 2010; published online 11 July 2010

References

1. Benoit, G., Hart, S. D., Temelkuran, B., Joannopoulos, J. D. & Fink, Y. Static and dynamic properties of optical microcavities in photonic bandgap yarns. *Adv. Mater.* **15,** 2053–2056 (2003).
2. Larsen, T. T., Bjarklev, A., Hermann, D. S. & Broeng, J. Optical devices based on liquid crystal photonic bandgap fibres. *Opt. Express* **11,** 2589–2596 (2003).

3. Benoit, G., Kuriki, K., Viens, J. F., Joannopoulos, J. D. & Fink, Y. Dynamic all-optical tuning of transverse resonant cavity modes in photonic bandgap fibers. *Opt. Lett.* **30,** 1620–1622 (2005).
4. Kerbage, C., Hale, A., Yablon, A., Windeler, R. S. & Eggleton, B. J. Integrated all-fiber variable attenuator based on hybrid microstructure fiber. *Appl. Phys. Lett.* **79,** 3191–3193 (2001).
5. Li, L., Wylangowski, G., Payne, D. N. & Birch, R. D. Broad-band metal glass single-mode fiber polarizers. *Electron. Lett.* **22,** 1020–1022 (1986).
6. Bergot, M. V. *et al.* Generation of permanent optically induced 2nd-order nonlinearities in optical fibers by poling. *Opt. Lett.* **13,** 592–594 (1988).
7. Townsend, P. D., Poustie, A. J., Hardman, P. J. & Blow, K. J. Measurement of the refractive-index modulation generated by electrostriction-induced acoustic waves in optical fibers. *Opt. Lett.* **21,** 333–335 (1996).
8. Fokine, M. *et al.* Integrated fiber Mach-Zehnder interferometer for electro-optic switching. *Opt. Lett.* **27,** 1643–1645 (2002).
9. Carpi, F. & De Rossi, D. Electroactive polymer-based devices for e-textiles in biomedicine. *IEEE Trans. Inf. Technol. Biomed.* **9,** 295–318 (2005).
10. Curie, J. & Curie, P. Développement par compression de l'électricité polaire dans les cristaux hémièdres à faces inclinées. *C. R. Acad. Sci. Paris* **91,** 294–295 (1880).
11. Arnau, A. *Piezoelectric Transducers and Applications* (Springer, 2008).
12. Abouraddy, A. F. *et al.* Towards multimaterial multifunctional fibres that see, hear, sense and communicate. *Nature Mater.* **6,** 336–347 (2007).
13. Kawai, H. Piezoelectricity of poly (vinylidene fluoride). *Jpn. J. Appl. Phys.* **8,** 975–976 (1969).
14. Lovinger, A. J. Ferroelectric polymers. *Science* **220,** 1115–1121 (1983).
15. Lando, J. B., Olf, H. G. & Peterlin, A. Nuclear magnetic resonance and X-ray determination of structure of poly(vinylidene fluoride). *J. Polym. Sci. A* **4,** 941–951 (1966).
16. Matsushige, K., Nagata, K., Imada, S. & Takemura, T. The ii-i crystal transformation of poly(vinylidene fluoride) under tensile and compressional stresses. *Polymer* **21,** 1391–1397 (1980).
17. Deng, D. S. *et al.* In-fiber semiconductor filament arrays. *Nano Lett.* **8,** 4265–4269 (2008).
18. Hart, S. D. *Multilayer Composite Photonic Bandgap Fibers* (Massachusetts Institute of Technology, 2004).
19. Furukawa, T. Ferroelectric properties of vinylidene fluoride copolymers. *Phase Transit.* **18,** 143–211 (1989).
20. Lando, J. B. & Doll, W. W. The polymorphism of poly(vinylidene fluoride). *J. Macromol. Sci.-Phys.* **B2,** 205–218 (1968).
21. Yagi, T., Tatemoto, M. & Sako, J. Transition behavior and dielectric-properties in trifluoroethylene and vinylidene fluoride co-polymers. *Polym. J.* **12,** 209–223 (1980).
22. Koga, K. & Ohigashi, H. Piezoelectricity and related properties of vinylidene fluoride and trifluoroethylene copolymers. *J. Appl. Phys.* **59,** 2142–2150 (1986).
23. Kimura, K. & Ohigashi, H. Ferroelectric properties of poly(vinylidenefluoride-trifluoroethylene) copolymer thin films. *Appl. Phys. Lett.* **43,** 834–836 (1983).
24. Eberhardt, F. J. & Andrews, F. A. Laser heterodyne system for measurement and analysis of vibration. *J. Acoust. Soc. Am.* **48,** 603–609 (1970).
25. Huber, R., Wojtkowski, M., Taira, K., Fujimoto, J. G. & Hsu, K. Amplified, frequency swept lasers for frequency domain reflectometry and OCT imaging: Design and scaling principles. *Opt. Express* **13,** 3513–3528 (2005).
26. Morrison, R. *Grounding and Shielding: Circuits and Interference* (IEEE Press, 2007).
27. Pinet, E. Medical applications: Saving lives. *Nature Photon.* **2,** 150–152 (2008).
28. Lurton, X. *An Introduction to Underwater Acoustics: Principles and Applications* (Springer, 2002).
29. Lines, M. E. & Glass, A. M. *Principles and Applications of Ferroelectrics and Related Materials* (Clarendon Press, 1977).
30. Neese, B. *et al.* Large electrocaloric effect in ferroelectric polymers near room temperature. *Science* **321,** 821–823 (2008).

Acknowledgements

The authors acknowledge A. F. Abouraddy, G. Benoit, M. Spencer, J. Rigling, M. Thompson, S. Griggs and J. F. Viens for their critical help and for discussions; S. A. Speakman for assistance with the XRD measurements; and E. L. Thomas for guidance. This work was supported in part by the Materials Research Science and Engineering Program of the US National Science Foundation under award number DMR-0819762, DARPA/Griggs and also in part by the US Army Research Office through the Institute for Soldier Nanotechnologies under contract no. W911NF-07-D-0004.

Author contributions

Y.F. and J.D.J. conceived the architecture of piezoelectric fibres. S.E., Z.W. and N.C. designed and fabricated fibre samples and carried out acoustic and heterodyne optical measurements. Z.W. constructed the acoustic transmission set-up. P.T.R. designed and constructed the heterodyne optical set-up. S.E. measured the Fabry–Perot/piezoelectric fibres. Z.M.R. and A.M.S. carried out thin-film deposition. D.S. carried out SEM imaging. S.E., Z.W., N.C., F.S., J.D.J and Y.F. co-wrote the manuscript.

Additional information

The authors declare no competing financial interests. Supplementary information accompanies this paper on www.nature.com/naturematerials. Reprints and permissions information is available online at http://npg.nature.com/reprintsandpermissions. Correspondence and requests for materials should be addressed to Y.F.